

# ***Covariance Data for Used Nuclear Fuel Uncertainty Analysis***

**Fuel Cycle Research & Development**

*Prepared for  
U.S. Department of Energy  
Campaign or Program  
M. T. Pigni and I. C. Gauld  
Oak Ridge National Laboratory  
March 2013  
FCRD-UFD-2013-000131*



**DISCLAIMER**

This information was prepared as an account of work sponsored by an agency of the U.S. Government. Neither the U.S. Government nor any agency thereof, nor any of their employees, makes any warranty, expressed or implied, or assumes any legal liability or responsibility for the accuracy, completeness, or usefulness, of any information, apparatus, product, or process disclosed, or represents that its use would not infringe privately owned rights. References herein to any specific commercial product, process, or service by trade name, trade mark, manufacturer, or otherwise, does not necessarily constitute or imply its endorsement, recommendation, or favoring by the U.S. Government or any agency thereof. The views and opinions of authors expressed herein do not necessarily state or reflect those of the U.S. Government or any agency thereof.

## ABSTRACT

The complete analysis of used nuclear fuel inventories to evaluate transportation and extended storage options require the calculation of the isotope inventories and radiological properties, and also their associated uncertainties. Recent advancements in the uncertainty information provided in basic nuclear cross-section data libraries, along with computational tools developed to apply these uncertainties in several distinct types of nuclear technology applications, have enabled accurate estimates of nuclear fuel properties and their uncertainties. In order to provide a comprehensive uncertainty analysis capability for used nuclear fuel analysis, one needs to further extend nuclear data uncertainties beyond cross-section data to include both fission product yields and nuclear decay data. The capability of propagation of basic nuclear data uncertainties provides a unique physics-based approach to uncertainty analysis that can be applied to fuel cycle studies and design concepts for scenarios where direct measurement data for validating the accuracy of modeling tools are neither available nor feasible (e.g., extended storage times). Application areas of uncertainty methods include nuclear decay heat, radiological source terms relevant to geologic disposal, and isotopic compositions relevant to burnup credit criticality analyses. This report describes the development of uncertainties and related correlations (covariance data) for independent fission product yields in the specific case of  $^{235}\text{U}$  at thermal neutron incident energy. Recent upgrades to the uncertainty analysis tools being developed to support implementation within the SCALE nuclear modeling and simulation code system are also described.



## CONTENTS

ABSTRACT.....	iii
1. INTRODUCTION.....	1
2. NUCLEAR DATA UNCERTAINTY ANALYSIS .....	2
2.1 What is Covariance (and why do we care)?.....	2
3. COVARIANCE DATA FOR FISSION PRODUCT YIELDS .....	3
3.1 Definition of independent yields.....	3
3.2 Model for Sum Yields.....	5
3.3 Model for Fractional Independent Yields .....	9
3.4 Model for Isomeric Yield Ratio .....	10
3.5 Determination of the Covariance Matrix .....	11
3.5.1 Bayesian method.....	12
4. COVARIANCES FOR NUCLEAR DECAY DATA .....	13
5. UNCERTAINTY EVALUATION TOOLS .....	13
6. BENCHMARKING THE NUCLEAR DATA AND METHODS .....	16
7. SUMMARY .....	16
Appendix A Model Parameters.....	18
A-1. Model Parameters for $Y(\mathbf{A})$ .....	18
A-2. Region Boundaries.....	18



## FIGURES

Figure 1. $^{235}\text{U}$ sum yields (in gray) and chain yields (in blue) of products of fission induced by thermal neutrons in linear (right labeling) and logarithmic scale (left labeling). The sum yields were computed via Eq. (2.4) using the independent yields from the chain yields were taken from the England and Rider compilation [1].	7
Figure 2. Ratio to ENDF/B-VII.1 of $^{235}\text{U}$ sum yields at thermal neutron incident energy taken from the England and Rider compilation [1] (in blue).	7
Figure 3. $^{235}\text{U}$ sum yields at thermal neutron incident energy plotted in linear (right labeling) and logarithmic scale (left labeling). The fit of $^{235}\text{U}$ sum yields at thermal neutron incident energy to 5 Gaussian model (in red) is compared to the ENDF/B-VII.1 evaluation and the sum yields calculated from Gaussian parameters before the fit (in black).	8
Figure 4. Ratio to ENDF/B-VII.1 of $^{235}\text{U}$ at thermal neutron incident energy taken from the England and Rider compilation [1] (in blue) and sum yields calculated with the set of parameters calculated from the fitting procedure (in red).	8
Figure 5. $^{235}\text{U}$ sum yield correlation matrix at thermal neutron incident energy.	9
Figure 6. $^{235}\text{U}$ independent fission yield correlation matrix at thermal neutron incident energy.	12
Figure 7. Plot showing the results of 500 criticality calculations performed by stochastic sampling of the nuclear cross section data.	15
Figure 8. $F_Z$ (in solid black) and $F_{A-Z}$ (in dashed red) functions for $^{235}\text{U}$ for excitation energy $E_c \leq 8$ MeV. Highlighted (in gray) are the wing and symmetry boundary regions.	21
Figure 9. $\sigma_Z$ function for $^{235}\text{U}$ for excitation energy $E_c \leq 8$ MeV. Highlighted (in gray) are the wing and symmetry boundary regions.	22
Figure 10. $\Delta Z$ function for $^{235}\text{U}$ for excitation energy $E_c \leq 8$ MeV. Highlighted (in gray) are the wing and symmetry boundary regions.	24

## TABLES

Table A.1. Parameters and related uncertainties defining the 5 Gaussian model for $Y(\mathbf{A}; \boldsymbol{\mu})$ .	18
Table A.2. Values of the average number of nucleons emitted before and after fission calculated by the equation for $\nu(E_c, Zf; p)$ for different fissioning nuclei at several neutron incident energies.	19
Table A.3. Parameters and related uncertainties defining the functions for $FA$ and $FA - Z$ for $^{235}\text{U}$ at thermal neutron incident energy.	20
Table A.4. Parameters and related uncertainties defining the functions for $\sigma_Z$ in the case of $^{235}\text{U}$ at thermal neutron incident energy. The excitation energy used for <b>sZ140</b> is $E_c = 7.59$ MeV.	22
Table A.5. Parameters and related uncertainties defining the functions for $\Delta Z$ in the case of $^{235}\text{U}$ at thermal neutron incident energy.	23





# USED FUEL DISPOSITION CAMPAIGN

## COVARIANCE DATA FOR USED NUCLEAR FUEL UNCERTAINTY ANALYSIS

This letter report was prepared under task Activity FT-13OR0810012, Quantify Sensitivities and Uncertainties in UNF Characteristics, and is the deliverable for subtask M4FT-13OR0810013, Covariance Files for Nuclear Data Uncertainty Analysis.

### 1. INTRODUCTION

One of the primary challenges facing the nuclear industry today is transportation and storage of high burnup (>45 GWd/MTU) (Ref. ISG-11) fuel. Analyses of engineering design and fuel cycle options require an accurate assessment of subcriticality margins, isotopic composition, dose levels, and decay heat over a long time period spanning onsite storage, transportation in shipping casks, and ultimate disposal at a repository—as well as potential reprocessing operations. Complete nuclear engineering analysis of systems for Used Nuclear Fuel (UNF) requires the calculation of the UNF values of interest and also the assessment of the uncertainties in calculated quantities associated with the basic nuclear data (fission product yields, decay constants, energy emission, etc.) used in the calculation. These uncertainties may directly impact the nuclear system performance, safety, and economic margins.

Recent developments in nuclear data uncertainty analysis have included considerable improvements in the representation and completeness of data uncertainties as well as major advances in the simulation tools required to use these uncertainties to nuclear technology applications. The increased interest in nuclear data uncertainty analysis lies in the ability to accurately predict system uncertainties based only on the uncertainties of the nuclear data used in the simulation, potentially reducing the reliance on large-scale experiments to measure nuclear fuel properties and characteristics for the purposes of code validation. In the area of UNF studies, this capability has an added benefit of providing uncertainties for extended nuclear fuel storage, transportation, and final disposition, in time regimes where measurements are not possible, e.g., times beyond about 50 years; and for advanced fuel cycle concepts where no measurements exist.

In the area of modeling and simulation of UNF, a large database of nuclear data libraries is utilized. In addition to the cross sections that define the nuclear transmutation reactions, a large set of radioactive decay data and fission product yield data are needed. Currently, evaluated nuclear data files contain cross section covariance data (uncertainties and their correlations) for a large set of the most important nuclides but do not include covariance information for fission product yields and nuclear decay data. For extended nuclear fuel storage applications, the importance of decay data increases as the concentrations and activities of radionuclides that are defined by their half-lives and decay chains. Any analysis of fission product uncertainties will also require complete uncertainty information on their production by fission.

One of the main objectives of this task is to develop covariance data for fission product yields and nuclear decay and, ultimately, to provide the capability to assess the impact of uncertainties in evaluated nuclear data files on engineered nuclear systems studies, such as UNF analysis. This interim letter report provides a detailed technical description of the development of fission product yield covariance data and summarizes recent advances in the uncertainty evaluation methodology which aim at an improved quantification of uncertainties associated with the analysis of engineering systems for UNF studies. Equally important to this project is the expansion of uncertainty evaluation tools to facilitate the regular use of these covariances in standard problems. In this report, recent development of a complete Monte Carlo based evaluation tool and progress towards its implementation in the SCALE code system are discussed along with plans for data and methods testing and validation.

## 2. NUCLEAR DATA UNCERTAINTY ANALYSIS

The computational methods used most widely in the U.S. for comprehensive used fuel inventory calculations include the ORIGEN and CINDER codes. Although the mathematical solutions used by these codes are different, the nuclear data requirements are the same. Accurate solutions of the time-dependent nuclide concentrations require nuclear data for

- neutron cross sections (reaction transmutation)
- fission product yields (formation of fission products via the fission process)
- and nuclear decay data (half-lives, branching fractions, energy release per decay)

Modern nuclear fuel isotopic modeling and simulation codes currently track a minimum of about 2200 individual nuclides generated by transmutation, fission, and decay. With consideration of all decay paths, nuclear reaction processes, and fission product yields for more than 1200 fission products and more than 30 fissionable nuclides, the system of nuclide fields can involve more than 40,000 transitions. Every transition is defined by nuclear data, and each nuclear data value has an associated uncertainty. Validation of these codes for UNF analyses is challenging due to the complexity of the nuclide systems and the time-dependent behavior of the nuclide compositions and fuel properties. Integral measurements designed for code validation are frequently not available for the fuel designs or cooling time range of interest.

The application of nuclear data uncertainty methods represents an approach for UNF systems uncertainty analyses. Such an approach has been demonstrated and applied to the area of burnup credit to evaluate the uncertainties in nuclear criticality safety calculations due to minor actinides and fission products present in irradiated fuel, but are not present in the current set of available criticality benchmark experiments. The estimation of  $k_{\text{eff}}$  uncertainties based on nuclear cross section uncertainties has been accepted as a technical basis for validating burnup credit nuclear criticality calculations by the Nuclear Regulatory Commission (e.g., NUREG/CR-7109, and NRC Interim Staff Guidance ISG-8 rev. 3).

The majority of international research effort in uncertainty analysis has been directed at expanding the data for nuclear cross-section uncertainties. The most recent release of the Evaluated Nuclear Data Files, ENDF/B-VII.1, provides extensive data on cross section uncertainties (covariance data evaluations) for 190 isotopes that are particularly important in nuclear technology applications. The previous release, ENDF/B-VII.0, contains neutron cross section covariances for 26 materials, of which only 14 were complete. The expansion of neutron cross section uncertainties represents one of the major advances in the new nuclear data library.

However, ENDF/B-VII.1 files (and other international evaluated nuclear data files) do not include complete uncertainty information for nuclear decay data or fission product yield data. These files contain uncertainties, but not the correlation (covariance) information necessary to apply the data to total system uncertainty analysis. Thus, new covariance data for radioactive decay and fission yields are being developed under this task and will be processed for use in the ORIGEN isotope generation and decay code to calculate their impact on UNF systems for storage, transportation, and repository studies. This capability will provide a complete uncertainty evaluation methodology for fuel inventory calculations performed by using the SCALE code.

### 2.1 What is Covariance (and why do we care)?

Uncertainties provided for nuclear data are generally defined by the accuracy of the experimental measurement. In the case of uncertainties for fission product yields found in current evaluated nuclear

data libraries, the uncertainty information includes the variance of the yield values for each fission product. However, variances alone are not sufficient for complete uncertainty assessment of complex systems. In addition to the data variances, covariances that describe correlations between different variables (in this case fission yields) are required. The correlations describe positive or inverse relationships in the data, and can arise from systematic uncertainties in the measurements or systematic behavior of the system being measured. The covariance describes how different variables move together as a group (correlated), or move in opposite directions (anti-correlated). Covariance data are frequently compiled in the form of matrices that include the quadratic sum of the statistical and systematic uncertainties (variances) on the diagonal elements, while on the off-diagonal elements included correlations between data. Covariance data for fission product yields are not available in current evaluated nuclear data files.

As an illustration of data correlations, fission product yields are defined such that they sum to 2.0, i.e., there are exactly two atoms produced per fission. Varying fission product yields independently to reflect the uncertainty in the yield values can easily result in a sum that is not 2.0, violating a basic constraint. Therefore, increasing the fission yield for one nuclide must also be accompanied by a reduction in the fission yields of one or more other nuclides. The inter-dependency of the yields is defined by the covariance matrix and can be estimated either by constraints or by nuclear model parameters used to represent the behavior of the data for complex processes.

Uncertainty analyses performed without accounting for the correlations in the data can lead to incorrect results – either an overestimation or underestimation of uncertainties, depending on the correlations. There, an accuracy assessment of the uncertainties in such systems therefore requires accurate and complete covariance data.

However, it is rather difficult to find published experimental data with an explicitly given covariance matrix. Hence, data evaluators must reconstruct the covariance matrix from the details of the experiments. In the present work the goal is to compute correlation matrices for (independent) fission yields on the base of the nuclear data in ENDF/B-VII.1 evaluation.

### 3. COVARIANCE DATA FOR FISSION PRODUCT YIELDS

Covariance data for fission product yields are not currently available in evaluated nuclear data files. This section provides a technical description of work performed under this task to develop the correlations and covariance matrix files required for fission product uncertainty analysis.

#### 3.1 Definition of independent yields

The independent yield  $y$  is the number of atoms of a fission product nuclide directly produced by a single fission after the emission of prompt neutrons, but before the emission of delayed neutrons. The independent fission product yields can be calculated from the sum yield  $Y$  and the fractional independent yield  $f$  by the relation

$$y(A, Z, I; \vec{\xi}) = Y(A; \vec{\xi})f(Z, A; \vec{\xi})R(A, Z, I; \vec{\xi}), \quad (3.1)$$

where  $R$  is the correction term for the isomeric yield ratio. Each independent yield is specified by the triplet  $A, Z, I$  where  $A$  and  $Z$  are the mass and atomic number, respectively, while  $I$  represents the isomeric state ( $I = 0$  for the ground state,  $I = 1, 2, \dots$  for the  $1^{st}, 2^{nd}, \dots$  excited states). The quantity  $\vec{\xi} = \{A_f, Z_f, E_n\}$  refers to the mass and atomic number of the fissioning nucleus denoted by  $A_f$  and  $Z_f$ , respectively. For neutron-induced fission the energy  $E_n$  is positive and  $A_f = A_{target} + 1$  is the compound

fissioning nucleus, while for spontaneous fission,  $E_n = 0$  and  $A_f$  is the mass number of the fissioning nuclide. Omitting the variable  $\xi$  the unitary condition of the fractional yields,

$$\sum_Z f(A, Z) = 1 \quad \forall A, \quad (3.2)$$

and of the isomeric yield ratios,

$$\sum_I R(A, Z, I) = 1 \quad \forall A, Z, \quad (3.3)$$

implies the sum of all independent yield of mass number  $A$  equals the sum yield  $Y(A)$ ,

$$\sum_{ZI} y(A, Z, I) = Y(A) \quad \forall A. \quad (3.4)$$

We note that, with the exception of delayed neutron ( $\beta^-, n$ ) emissions and the very few long-lived  $\alpha$  decays, all fission products decays through isomeric transitions or  $\beta^\pm$  modes for which the mass number  $A$  is unaltered. Thus, to a very good approximation, the fission products can be considered as belonging to distinct mass chains and, conveniently expressed by Eq. (3.4).

In addition, independent yield data must satisfy three conditions. First, the total yield must be normalized to 2 (two fragments per fission)

$$\sum_{AZI} y(A, Z, I) = 2, \quad (3.5)$$

where the index runs over each fission. The condition in Eq. (3.5) is automatically fulfilled when the unitary conditions of Eqs. (3.2)-(3.3) are satisfied and the total sum yield is constrained to

$$\sum_A Y(A) = 2,$$

where the index runs over each fission products with the same mass.

Second, the total mass must be the mass of the fissioning compound nucleus minus the average total number of nucleons  $\nu$  emitted before and after fission,

$$\sum_{AZI} A y(A, Z, I) = A_f - \nu,$$

or equivalently,

$$\sum_{AZ} A Y(A) = A_f - \nu.$$

For high-energy neutron induced fission, the quantity  $\nu$  also needs to include the pre-fission neutrons since nucleons may be emitted before fission during de-excitation of a highly excited nucleus. For instance, above the threshold of first chance fission, there are two fissioning compound nuclei,  $A_f$  and  $A_f - 1$ . For excitation energy  $E_c \lesssim 8$  MeV or for neutron incident energy  $E_n \lesssim 2$  MeV, it is a good approximation to assume  $\nu$  as the average number of the prompt fission neutrons,  $\nu_F$ , as described in the appendix.

The third condition is placed on the total charge that must be the same as that of the fissioning nucleus

$$\sum_{AZI} Z y(A, Z, I) = Z_f,$$

or equivalently,

$$\sum_{AZ} Z Y(A) f(A, Z) = Z_f.$$

### 3.2 Model for Sum Yields

We modeled the sum yields by the use of a set of five Gaussians. By assuming symmetry and requiring a total sum yield of 2, the five Gaussian model uses a total of 8 independent parameters, to represent the sum yield as

$$Y(A) = \sum_{i=1}^2 N_i (\psi_i^+ + \psi_i^-) + N_3 \psi_3,$$

where

$$\psi_i^\pm(A) = (\sqrt{2\pi}\sigma_i)^{-1} e^{-(A-\bar{A} \pm D_i)^2 / 2\sigma_i^2}$$

and

$$\psi_3^\pm(A) = (\sqrt{2\pi}\sigma_3)^{-1} e^{-(A-\bar{A})^2 / 2\sigma_3^2}.$$

$N_i$  is the normalization factor of the  $i^{th}$  Gaussian and  $\sigma_i$  its width parameter.  $\bar{A}$  is the mean mass of the distribution and  $D_i$  is the separation of the  $i^{th}$  Gaussian peak from  $\bar{A}$ . The mean mass distribution can be also written as a function of the average total number of nucleons emitted, namely,  $\bar{A} = (A_f - \nu)/2$ . In order to guarantee the sum yields sum to 2, the normalization factor of  $\psi_3$  is defined as

$$N_3 = 2(1 - N_1 - N_2).$$

In Fig. 1 we plot the sum yields for  $^{235}\text{U}$  computed via Eq. (2.4) where the independent yields and related uncertainties were taken from the ENDF/B-VII.1 evaluation. In this evaluation there is a total number of 107 chain masses with mass numbers between  $A_{min} = 66$  and  $A_{max} = 172$ . The results are compared to the chain yields,  $C(A)$ , taken from the England and Rider compilation [1]. In both chain and sum yields one can note some kind of asymmetry between fission products with low and high mass numbers. The sum yield  $Y(A)$  and the chain yield  $C(A)$  for a mass chain  $A$  may differ by a few percent, because the latter applies after delayed neutron emissions. The chain yield  $C(A)$  is the sum of all cumulative yields  $c(A, Z, I)$  that are stable or has a very long half-life,

$$C(A) = \sum_i^N c_i \delta(A = A_i) \delta(T_{1/2} \gg T_\infty),$$

where the cumulative yields for  $A = A_i$  are defined in the infinite time domain after the independent yields are produced, namely,

$$c_i = y_i + \sum_j c_j b_{ji},$$

where the branching ratio to the mass number  $A_i$  satisfies the normalization condition  $\sum_j b_{ji} = 1$ .

Figure 2 shows for each chain mass  $A$  the ratios of the chain yield to ENDF/B-VII.1 sum yield of the fission products of induced by thermal neutron fission (0.0253 eV) for  $^{235}\text{U}$ . With the exception of small differences in the mass region between  $A = 80 - 90$  and  $A = 130 - 140$ , the agreement between sum and chain yields is within  $< 1\%$ . In Fig. 3 we show the fit (in red) of ENDF/B-VII.0 sum yields for  $^{235}\text{U}$  thermal fission using the 5 Gaussian model. It is also shown (in black) the sum yields calculated using the 5 Gaussian model with an initial set of parameters taken from [2]. The uncertainties for the ENDF/B-VII.1 sum yields used in the fitting procedure were computed as quadratic summation of the uncertainties of independent fission yields provided in the ENDF/B-VII.1 evaluation. As one can notice, the fitted sum yield (red solid line) shows significant differences in the peak regions with respect to the initial curve (black solid line). This is due to two main reasons. The first one is related to the relative high uncertainties of the data used in the fitting procedure, while the second one derives from the symmetry imposed by the 5 Gaussian model between the peak regions. The model is symmetric with respect to the mean mass of the distribution and, since symmetry cannot be achieved experimentally, this can be viewed as a limitation in reproducing the data used in the fitting procedure.

The quality of the fitting is shown in Fig. 4 where the ratio to ENDF/B-VII.1 of sum yields computed by the 5 Gaussian model. Although the high degree of symmetry between the fission products with low and high mass numbers on which the 5 Gaussian model is defined, the differences are within the uncertainties of the data used in the fitting procedure. Figure 5 shows the correlation matrix of the  $^{235}\text{U}$  sum yields at thermal neutron energy. Correlations close to 1 are seen in the symmetry region ( $A \approx 118$ ) and in the wing regions ( $A \approx 60$  and  $A \approx 160$ ) while negative correlations are present in the peak regions ( $A \approx 100$  and  $A \approx 140$ ). This is due to the definition of the normalization constant  $N_3$ , which constrains the total sum yield. The correlation matrix is by definition symmetric and, due to model, one can also see some degree of symmetry between the axes of non-diagonal elements. Quite large portions of the matrix have correlations close to zero, while strong negative correlations are seen in the low and high peak regions along the diagonal.

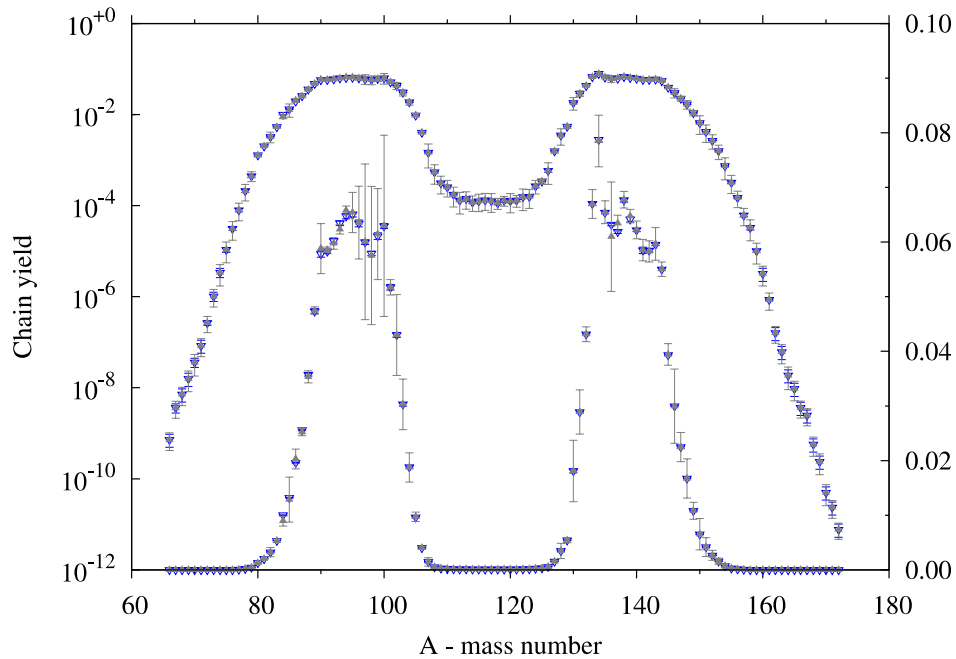


Figure 1.  $^{235}\text{U}$  sum yields (in gray) and chain yields (in blue) of products of fission induced by thermal neutrons in linear (right labeling) and logarithmic scale (left labeling). The sum yields were computed via Eq. (3.4) using the independent yields from the chain yields were taken from the England and Rider compilation [1].

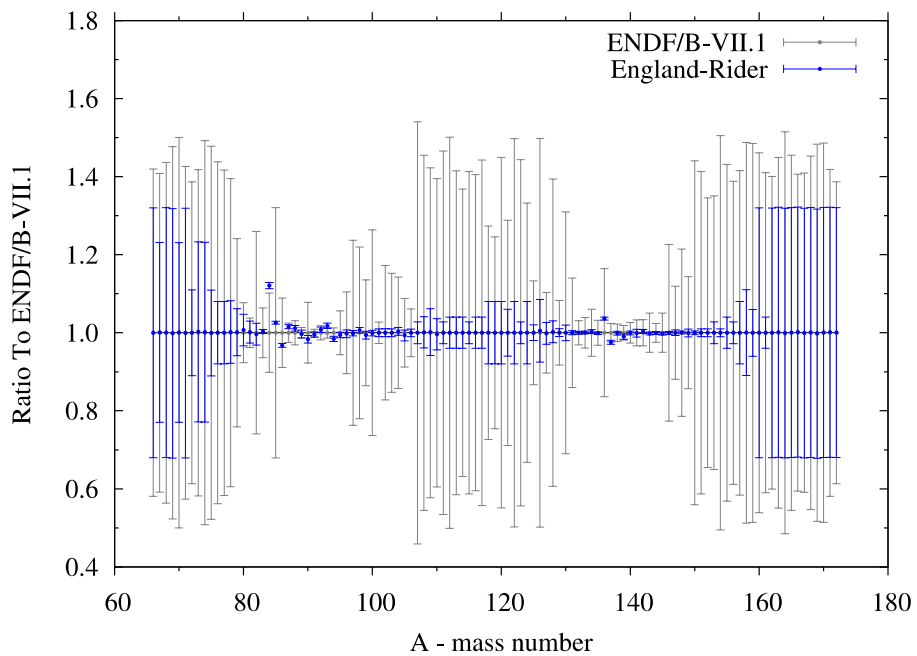


Figure 2. Ratio to ENDF/B-VII.1 of  $^{235}\text{U}$  sum yields at thermal neutron incident energy taken from the England and Rider compilation [1] (in blue).

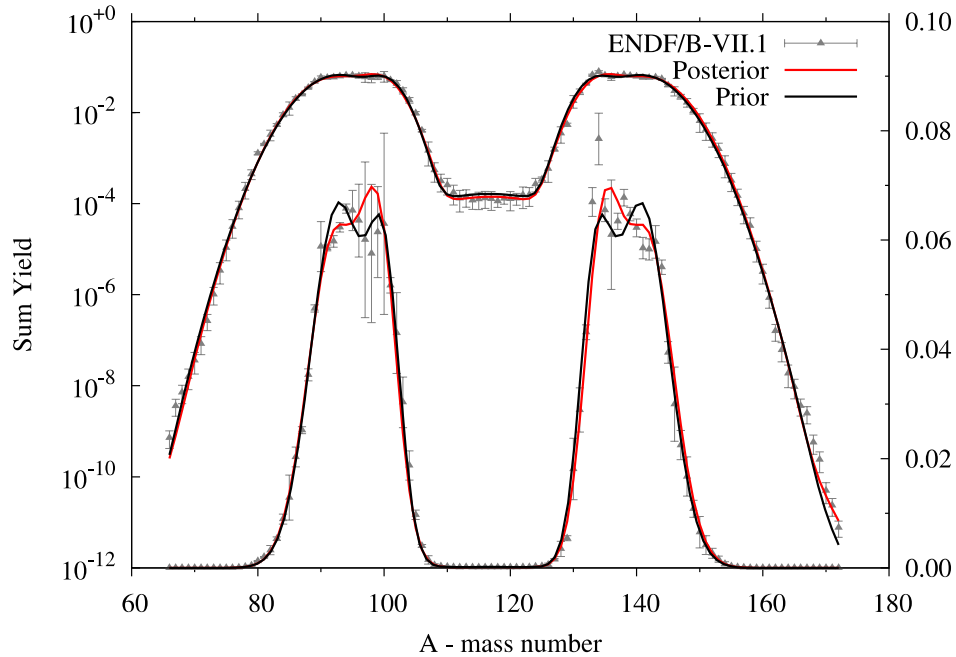


Figure 3.  $^{235}\text{U}$  sum yields at thermal neutron incident energy plotted in linear (right labeling) and logarithmic scale (left labeling). The fit of  $^{235}\text{U}$  sum yields at thermal neutron incident energy to 5 Gaussian model (in red) is compared to the ENDF/B-VII.1 evaluation and the sum yields calculated from Gaussian parameters before the fit (in black).

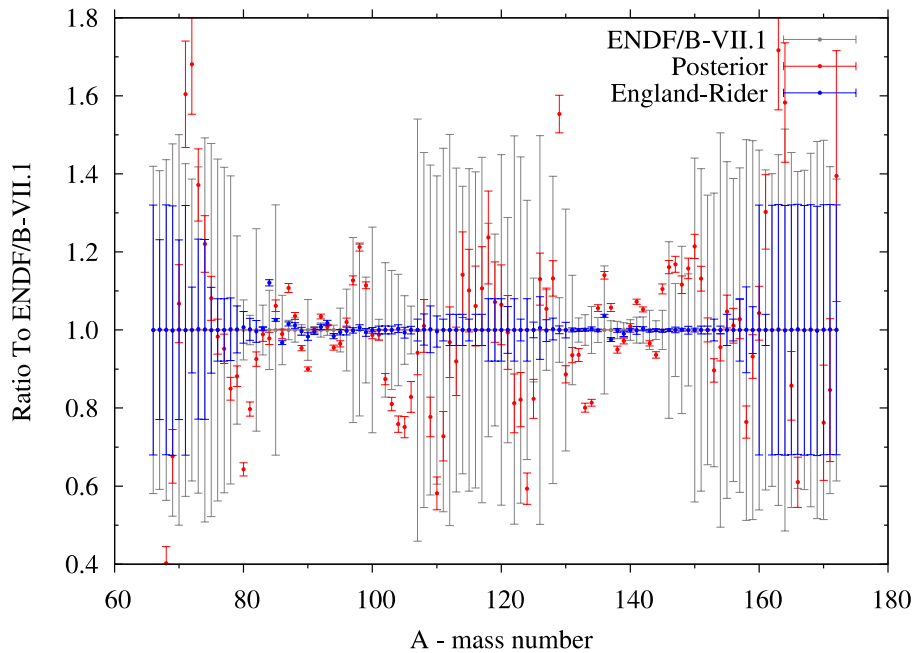


Figure 4. Ratio to ENDF/B-VII.1 of  $^{235}\text{U}$  at thermal neutron incident energy taken from the England and Rider compilation [1] (in blue) and sum yields calculated with the set of parameters calculated from the fitting procedure (in red).



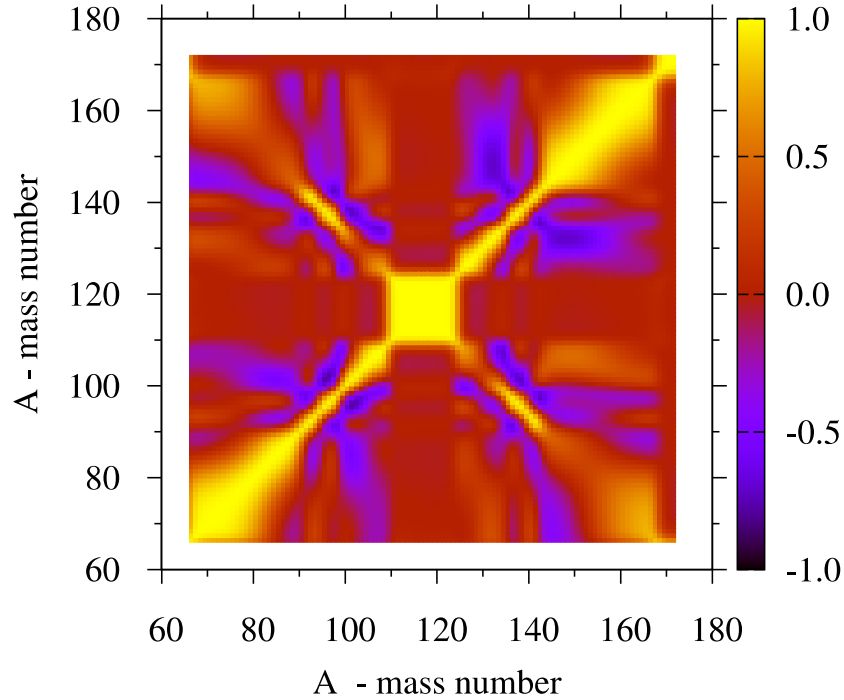


Figure 5.  $^{235}\text{U}$  sum yield correlation matrix at thermal neutron incident energy.

### 3.3 Model for Fractional Independent Yields

The fractional independent yields were calculated by the  $Z_p$  model developed by Wahl [3]. The  $Z_p$  is a (semi)empirical model that defines the independent fractional yields as Gaussian distribution in mass and charge respectively, modified by an odd-even effect as

A

$$f(A, Z) = \frac{1}{2} N(A) F(A) \left( \sqrt{\frac{\pi}{2}} \sigma_z \right)^{-1} \int_{Z-1/2}^{Z+1/2} e^{-\frac{(Z'-Z_p)^2}{2\sigma_z^2}} dZ',$$

where the last term can be given in terms of the error functions of

$$V = \frac{Z - Z_p + 1/2}{\sigma_z \sqrt{2}} \quad \text{and} \quad W = \frac{Z - Z_p - 1/2}{\sigma_z \sqrt{2}},$$

$$\left( \sqrt{\frac{\pi}{2}} \sigma_z \right)^{-1} \int_{Z-1/2}^{Z+1/2} e^{-\frac{(Z'-Z_p)^2}{2\sigma_z^2}} dZ' = \text{erf}(V) - \text{erf}(W).$$

The most probable charge on mass number  $A$

$$Z_p(A) = (A + \nu_p) \frac{Z_p}{A_f} + \Delta Z$$

accounts for the average number of post fission neutrons emitted to form fission products with mass number  $A$  by the function  $\nu_p \equiv \nu_p(A)$ , while the mean charge of the distribution is corrected by the function  $\Delta Z \equiv \Delta Z(A + \nu_p)$ . Both functions and their parameters are described in the appendix as well as the width of the Gaussian distribution  $\sigma_z \equiv \sigma_z(A + \nu_p)$ . The normalization factor  $N(A)$  is applied in order to achieve the unitary condition of the fractional yields, i.e. Eq. (3.2), since the function  $F(A)$  for the even-odd effects in proton and neutron pairing (for details see appendix) destroys the inherent normalization properties of the Gaussian distributions.

### 3.4 Model for Isomeric Yield Ratio

We defined the isomeric yield ratio as described by Katakura in Ref. [4] where the function  $R(A, Z, I)$  is expressed by ratios,  $r(A; J_0, J_1)$  of ground state ( $I = 0$ ) and metastable ( $I = 1$ ) yield as

$$r(A; J_0, J_1) = \begin{cases} (1 + r(A; J_0, J_1))^{-1}, & I = 0 \\ (1 + r^{-1}(A; J_0, J_1))^{-1}, & I = 1 \end{cases}$$

where  $J_0$  and  $J_1$  are the spins of the nuclide (specified by mass number  $A$  and atomic number  $Z$ ) for the ground and metastable state, respectively. The ratios  $r(A; J_0, J_1)$  are defined through the Madland and England [5] functions  $F_i$  as

$$r(A; J_0, J_1) = \begin{cases} \frac{F_i(J_0, J_1)}{1 - F_i(J_0, J_1)}, & J_1 - J_0 > 0 \\ \frac{1 - F_i(J_0, J_1)}{F_i(J_0, J_1)}, & J_1 - J_0 < 0 \end{cases}$$

where the index  $i = 1, \dots, 4$  and the  $F$  functions are defined for odd- $A$  nuclides with  $|J_1 - J_0| = \text{even}$  and  $|J_1 - J_0| = \text{odd}$ , respectively, by

$$F_1 = e^{1/\langle J^2 \rangle} \left\{ e^{-\frac{[J_0 + J_1 + 3]^2}{2\langle J^2 \rangle}} + \frac{J_0 + J_1 + 1}{2\langle J^2 \rangle} e^{-\frac{[J_0 + J_1 + 1]^2}{\langle J^2 \rangle}} \right\}$$

$$F_2 = e^{1/\langle J^2 \rangle} e^{-\frac{[J_0 + J_1 + 2]^2}{\langle J^2 \rangle}}$$

and for even- $A$  nuclides with  $|J_1 - J_0| = \text{even}$  and  $|J_1 - J_0| = \text{odd}$ , respectively, by

$$F_3 = e^{-\frac{(J_0 + J_1 + 2)(J_0 + J_1 + 4)/4}{\langle J^2 \rangle}} + \frac{J_0 + J_1 + 1}{2\langle J^2 \rangle} e^{-\frac{(J_0 + J_1)(J_0 + J_1 + 2)/4}{\langle J^2 \rangle}}$$

$$F_4 = e^{-\frac{(J_0+J_1+1)(J_0+J_1+3)/2}{\langle J^2 \rangle}}$$

The square root of the quantity  $\langle J^2 \rangle \equiv J_{rms}^2(E_n)$  is the angular momentum of the initial fragment and depends on the incident neutron energy  $E_n$ . For the present calculations we adopted  $J_{rms} = 7.5$ .

### 3.5 Determination of the Covariance Matrix

The analysis of the independent fission yields followed the procedure outlined in Section 3. In order to estimate the effect of the statistical and systematic uncertainties on the fission product yields we assumed the validity of linear error propagation. Let us denote the different sources of uncertainties that enter into the fission product yield determination with the vector  $\vec{x}$ . The covariance matrix is given by

$$\langle \Delta y_c \Delta y_{c'} \rangle = \sum_{k\ell} \frac{\partial y_c(\vec{x})}{\partial x_k} \langle \Delta x_k \Delta x_\ell \rangle \frac{\partial y_{c'}(\vec{x})}{\partial x_\ell},$$

where the index  $c(c')$  represents the triplet  $A, Z, I(A', Z', I')$  and  $\langle \Delta x_k | \Delta x_\ell \rangle$  is the covariance matrix of the model parameters.  $\partial y_c / \partial x_k$  is the partial derivative of the independent fission yield calculated at  $c \equiv (A, Z, I)$  with respect to the model parameter  $x_k$ . Essentially two sources of uncertainties have been taken into account. The first one derives from the set of 8 parameters  $\vec{\mu} \equiv \{N_1, \sigma_1, D_1, N_2, \sigma_2, D_2, \bar{A}, \sigma_3\}$ , that models the sum yield as explained in Sec. 3.2. The second component is related to the set of parameters,  $\vec{\lambda} \equiv \{\vec{f}_r, \vec{s}_r, \vec{d}_r\}$  defining the (semi)empirical  $Z_p$  model as described in Sec. 3.3. We assumed the parameters specifying the sum yields and the independent fractional yields are independent, so that one can express the overall covariance matrix of model parameters in terms of independent sub-matrices as

$$\langle \Delta x_k \Delta x_\ell \rangle \equiv \begin{pmatrix} \langle \Delta \mu_i \Delta \mu_{i'} \rangle & 0 \\ 0 & \langle \Delta \mu_j \Delta \mu_{j'} \rangle \end{pmatrix}.$$

The numerical values of the model parameters and their related uncertainties and correlations can be found in the appendix. In Fig. 6 we show the correlation matrix for independent fission yields on  $^{235}\text{U}$  at thermal incident neutron energy obtained with the procedure described above. The matrix has 975x975 elements arranged according the grid used in the ENDF/B-VII.1 evaluation. The numbers on the x- and y-axis denote the matrix elements associated with the triplet (A,Z,I). One can notice that the small and negative correlations are dominant and the pattern resembles in some way that one of the sum yield correlation matrix.

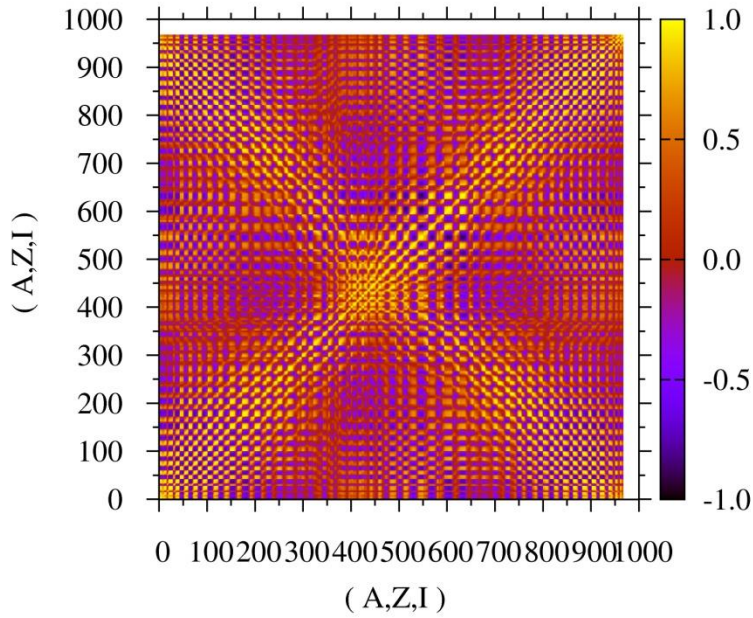


Figure 6.  $^{235}\text{U}$  independent fission yield correlation matrix at thermal neutron incident energy.

### 3.5.1 Bayesian method

In this section we describe the sequential Bayesian update procedure developed by T. Kawano at Los Alamos National Laboratory. The prior vector,  $y_0$ , is associated with the independent fission product yields and, when the evaluated sum/chain yield,  $Y$ , as well as the related covariance matrix,  $Z$ , are provided as new information, an updated  $y_1$  is given by

$$P_1 = P_0 - P_0 S^T (S P_0 S^T + Z)^{-1} S P_0,$$

$$y_1 = y_0 + P_1 S^T Z^{-1} [Y - F(y_0)],$$

where  $P_1$  is the updated covariance matrix of the independent fission yields and the matrices  $S$  and  $S^T$  are the sensitivity matrix of  $y_0$  and its transpose, respectively, whose matrix elements for a small perturbation  $\delta$  are given numerically by

$$S_{ij} \approx \frac{1}{2\delta} \{F_i(y_{0,1}, y_{0,2}, \dots, y_{0,j} + \delta, \dots) - F_i(y_{0,1}, y_{0,2}, \dots, y_{0,j} - \delta, \dots)\}.$$

The constraints on  $y_1$  can be added by similar equations. For the normalization of the total independent yield,

$$P_2 = P_1 - P_1 T^T (T P_1 T^T + \sigma_T^2)^{-1} T P_1,$$

$$y_2 = y_1 + P_2 T^T (\sigma_T^2)^{-1} [2 - T^T y_1],$$

where the  $N$  –dimensional unit vector  $T$  is defined such as  $T^T y_1 = \sum_i^N y_{1,i} = 2$  and the parameter  $\sigma_T$  controls how the integral goes close to 2.0. For the mass and charge conservation, the same sequence is repeated,

$$P_3 = P_2 - P_2 U^T (U P_2 U^T + \sigma_U^2)^{-1} U P_2,$$

$$y_3 = y_2 + P_3 U^T (\sigma_U^2)^{-1} [A_f - \nu - U^T y_2]$$

and

$$P_4 = P_3 - P_3 V^T (V P_3 V^T + \sigma_V^2)^{-1} V P_3,$$

$$y_4 = y_3 + P_4 V^T (\sigma_V^2)^{-1} [Z_f - V^T y_3],$$

where  $\sigma_U$  and  $\sigma_V$  are criteria to satisfy the following constraints,  $U^T y_2 = \sum_i^N y_{2,i} A_i = A_f - \nu$  and  $V^T y_3 = \sum_i^N y_{3,i} Z_i = Z_f$ , respectively.

#### 4. COVARIANCES FOR NUCLEAR DECAY DATA

Covariance data files are currently being prepared under this task for the analysis of nuclear decay data uncertainties. Similar to the status of the fission product yields in ENDF/B-VII, the evaluated nuclear data files contain decay data uncertainties but do not have the covariance information needed to accurately simulate the net impact of uncertainties from all nuclides in the system.

A review of the decay data however indicates that, unlike fission product yields, the correlations in decay data are expected to be very minor. In other words, the uncertainties in the half-life value for a given nuclide are not correlated with the uncertainties for any other nuclide. The exception could occur if the half-life of a nuclide was measured using another nuclide as a reference standard. However, these correlations are expected to be minor.

Correlations in the decay schemes do occur for nuclides that decay by more than one decay mode, e.g., isomeric transition and beta decay. Any error in one of the decay modes must be compensated in the other decay mode such that the branching fractions sum to 1.0, e.g., anti-correlated. Correlation in the branching fractions will be included in the decay data uncertainty analysis.

#### 5. UNCERTAINTY EVALUATION TOOLS

Covariance data represents an extremely large database of uncertainty information. Practical uncertainty evaluation tools are required to process this information and apply it to standard nuclear technology problems.

Tools for nuclear data uncertainty analysis exist in SCALE and have been demonstrated for application to nuclear criticality safety, where the methodology has been applied to calculate the k-eff uncertainties for a large set of critical experiments. This methodology is implemented in the TSUNAMI module and uses first-order perturbation theory to calculate nuclear data sensitivities (or cross section values to the k-eff value) and combines these sensitivities with a comprehensive cross section covariance file to determine the k-eff uncertainties for a wide variety of critical benchmark experiments. However, the perturbation theory approach cannot be applied to nuclear fuel isotopic depletion calculations where a large number of responses are of interest, and where the composition of the system (i.e., nuclear fuel) varies as a function of time due to nonlinear interactions between the neutron flux and nuclide concentrations.

Recently, development of alternate Monte Carlo-based uncertainty analysis methodology has been initiated for implementation in SCALE. This method performs a statistical sampling of the nuclear data based on covariances such that both the data uncertainty and the correlations between the data are accurately represented. The statistical Monte Carlo sampling of the nuclear data produces a randomly varied set of nuclear data libraries where the variations are representative of the uncertainties inherent in the nuclear data. Each library is then input to the SCALE computation sequences to obtain a randomly perturbed output response. The calculations are repeated, with each calculation using a different perturbed library until a sufficient number of data samples have been taken, statistical analysis provides the standard deviations in the desired output responses. Although computationally intensive, this approach allows uncertainty propagation in very complex computational problems to be performed, including reactor burnup calculations to obtain uncertainties in ANY time-dependent responses important for UNF transportation, storage, and disposal.

The sampling of the nuclear data covariance files is currently performed using the XSUSA code developed by Gesellschaft fuer Anlagen-und Reaktorsicherheit (GRS), in Germany. The XSUSA approach assumes that the nuclear data are random variables characterized by multivariate normal distributions that are defined by their mean (expected) values. A cross section covariance library is currently distributed in SCALE. At this time, only cross-section covariance data are available in SCALE and have been applied to statistical uncertainty sampling.

XSUSA uses an established methodology to propagate cross-section uncertainties and analyze their impact on reactor analysis. There have recently been significant advancements in the ENDF/B-VII evaluated nuclear data files to include extensive uncertainty and covariance data for cross section uncertainty analysis. However, the approach has not been expanded previously to perform complete uncertainty evaluations for all nuclear data used by reactor and nuclear fuel irradiation and decay codes. This limitation derives primarily from a lack of covariance data required for the propagation of fission yields and decay constant uncertainties, relevant to used fuel isotopic predictions.

The XSUSA procedure has been updated to perform uncertainty sampling for the fission yields and decay data using the new covariance information developed under this task. To provide users with access to this statistical sampling uncertainty methodology, a new control module, SAMPLER, is being developed. The SAMPLER code performs the function of automating the calculation procedure, each calculation executed using a new randomly perturbed data library, and compiles the results for statistical analysis of the output. The methods are being updated to support the SCALE depletion sequences that use the ORIGEN code to track the time-dependent nuclide concentrations in the fuel and calculate the fuel properties and radiological characteristics.

Significant development effort is currently underway to upgrade the SAMPLER tool to perform fission product yield uncertainty and decay data uncertainty Monte Carlo sampling. The most significant developments completed to date include

- re-writing the SAMPLER code in C++ to take advantage of cutting edge code architecture and SCALE infrastructure, with modular extensible layout, and multi-platform operability

- implemented parallel calculations using both MPI (cluster networks) and Open MP for multiprocessor systems
- user-requested responses can be defined to be obtained from the output file using regular `grep` expressions (functions on multi-platforms), the lattice physics `xfile016`, and the ORIGEN concentration file `ft71f001`
- response data are automatically extracted and statistical operations are performed (mean, variance, correlations)
- response data and statistics are also generated in standard table formats including text output, CSV files (for Excel compatibility), and plot data that can be viewed using Javapeno

An example of the current capability of the uncertainty analysis tool is illustrated in Fig. 1, showing the distribution of  $k$ -eff results for a critical system based on 500 criticality simulations using the KENO code. In each calculation, the all cross sections are varied based on the covariance data (uncertainties and correlations) within the uncertainty of the evaluated cross section data. The  $k$ -eff results can then be statistically evaluated to determine the uncertainty in the criticality calculation, and parameters such as the one-sided 95% upper tolerance limit (widely used criterion in nuclear safety studies).

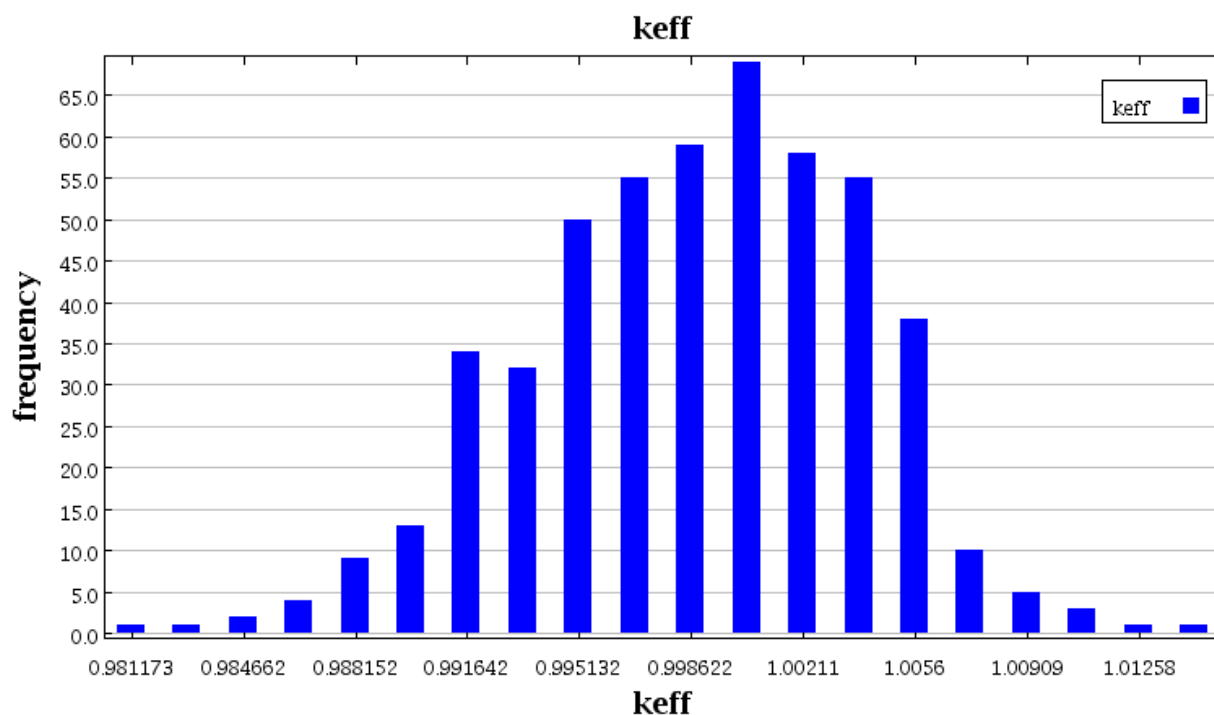


Figure 7. Plot showing the results of 500 criticality calculations performed by stochastic sampling of the nuclear cross section data.

## 6. BENCHMARKING THE UNCERTAINTY METHODS

Although benchmarking and validation of the data and methods has not been initiated, some of the initial benchmark activities are briefly discussed. These activities will be performed to validate both the covariance data developed in this task and the stochastic uncertainty sampling methods used to apply the covariance data to UNF modeling and simulations. Validation and testing activities will include:

- Analyses using independent approaches to covariance data model development described in this report, using the Wahl and the Kawano methods. The latter model was developed at LANL and used to generate fission product yields for  $^{239}\text{Pu}$  in ENDF/B-VII.1.
- Evaluation of decay heat and uncertainties at long cooling times using values and uncertainties from ANS-5.1-2005 standard.
- Evaluation of decay heat values and uncertainties using experimental data for more than 60 spent fuel assemblies measured at the Swedish Interim Storage Facility for Spent Nuclear Fuel for cooling times up to about 30 years (a collaboration with ORNL).
- Analysis of uncertainties compared to experimental measurements at short cooling times after fission (1 second to about 8 hours).
- Application to the analysis of uncertainties in calculated nuclide inventories using comparisons with destructive radiochemical analysis of nuclide concentrations.

## 7. SUMMARY

This report presents the status of task Activity FT-13OR0810012; Quantify Sensitivities and Uncertainties in UNF Characteristics. Development of covariance data for fission product yields, Milestone M4FT-13OR0810013; Covariance Files for Nuclear Data Uncertainty Analysis, is complete and is the subject of this report.

The work performed in this task is one of the first applications of the statistical uncertainty sampling method to include nuclear decay data (half-lives, branching fraction, and energy release per decay) and fission yields. This extension of the uncertainty capability allows uncertainties to be calculated for actinide and fission product isotopes, decay heat, and activities, and integral quantities such as the neutron multiplication factor (nuclear criticality safety) — all of which depend on the nuclear data uncertainties of many fission products and actinides. This work includes the development of nuclear data correlations (covariance) required to perform uncertainty studies and the evaluation tools necessary to handle the large amounts of nuclear data and results from the many calculations performed as part of this approach.

Significant progress has been made in the upgrade of the uncertainty evaluation tools required to apply uncertainty information to standard nuclear analysis problems. These upgrades are included in the SAMPLER code developed for automated stochastic sampling of uncertainties for application to standard calculations performed in the SCALE code system.

Covariance data for fission product yields and decay data has not been widely available or used in practical applications. It is important to note that covariance evaluation methodologies in this area are novel approaches to uncertainty analysis, and a consensus within the nuclear data community on the most reliable approach has not been reached.

There is considerable interest in this field of research within the international nuclear data community, particularly for applications to advanced fuel cycle uncertainty analysis. In particular, the European Community has established a multi-year nuclear project called ANDES that includes tasks to evaluate uncertainties and covariances in fission product yields. Another important international activity in this area in the OECD Nuclear Energy Agency working group on Uncertainty Analysis Methods (UAM).



Although this group is primarily interested in the evaluation of uncertainties due to cross sections, their work is expanding to include depletion of used fuel and associated uncertainties in nuclide concentrations. Lastly, the OECD has also recently initiated a new subgroup under the Working Party on International Nuclear Data Evaluation Co-operation (WPEC) on fission product yield uncertainties – WPEC-37. Continued liaison with this WPEC-37 is viewed as an important activity for this project to ensure international experience on this complex topic is incorporated into uncertainty studies for the UFD and as a means to benchmark our findings with those obtained using alternate approaches.

## 8. REFERENCES

- [1] T. R. England and B. F. Rider, "ENDF-349 Evaluation and Compilation of Fission Product Yields," Technical Report LA-UR-94-3106, Los Alamos National Laboratory (1994).
- [2] M. F. James, R. W. Mills, and D. R. Weaver "A New Evaluation of Products Yields and the Production of a new Library (UKFY2) of Independent and Cumulative Yields," *Prog. Nucl. Energ.*, 26, 1 (1991).
- [3] A. C. Wahl, "Systematics of Fission-Product Yields," Technical Report LA- 13928, Los Alamos National Laboratory (2002).
- [4] J. Katakura, "JENDL FP Decay Data File 2011 and Fission Yields Data File 2011," JAEA-Data/Code 2011-25, Japan Atomic Energy Agency (2012).
- [5] D. G. Madland and T. R. England, "Distribution of Independent Fission Product Yields to Isomeric State," LA-6595-MS, Los Alamos National Laboratory (1976).

## Appendix A

### Model Parameters

#### A-1. Model Parameters for $Y(A)$

In Tab. A.1 gives the set of parameters that defines the sum yield  $Y(A; \vec{\mu})$ . The parameter uncertainties and related correlations are also shown

Table A.1. Parameters and related uncertainties defining the 5 Gaussian model for  $Y(A; \vec{\mu})$

Name	$\vec{\mu}$	$\Delta\vec{\mu}$	Error(%)	Correlation Matrix			
$N_1$	0.6267	$8.71 \cdot 10^{-3}$	1.39	1.000			
$\sigma_1$	4.1430	$2.36 \cdot 10^{-2}$	0.57	0.817	1.000		
$D_1$	24.750	$8.16 \cdot 10^{-2}$	0.33	-0.891	-0.864	1.000	
$N_2$	0.3716	$8.69 \cdot 10^{-3}$	2.34	-1.000	-0.816	0.891	1.000
$\sigma_2$	2.7670	$3.76 \cdot 10^{-2}$	1.36	-0.741	-0.569	0.698	0.742
				1.000			
$D_2$	17.530	$7.36 \cdot 10^{-2}$	0.42	-0.847	-0.643	0.767	0.847
				0.781	1.000		
$\bar{A}$	116.90	$2.33 \cdot 10^{-2}$	0.002	-0.092	-0.177	0.296	0.092
				0.153	0.059	1.000	
$\sigma_3$	9,6190	$7.40 \cdot 10^{-2}$	0.77	0.045	0.030	-0.071	1.000

#### A-2. Region Boundaries

As described in Ref. [3], the (semi)empirical  $Z_p$  model uses the parameters  $\Delta Z, \sigma_z, F$  to compute the independent fractional yields. These parameters can be represented by simple functions which depend on  $A' \equiv A + \nu_p$  and which are defined in region boundaries of  $A'$ . The region boundaries used in this work are  $\vec{b} = \{70, 77, 105.7, 111.2, 124.8, 130.3, 159, 166\}$ . The regions for  $A' \in (b_1, b_2)$  and  $A' \in (b_7, b_8)$  are usually referred as wing regions whereas those ones for  $A' \in (b_2, b_3)$  and  $A' \in (b_5, b_6)$  as peak regions. The symmetry region is for  $A' \in (b_3, b_4)$ .

#### A-3. Model for Average Number of Nucleons

The following equations describe the parameterization of the average number of nucleons emitted before and after fission as defined by Wahl [3],

$$\nu(E_c, Z_f; \vec{p}) = \begin{cases} p_2 - [p_2 - p_1 - p_0(Z_f - 92)]e^{-p_3 E_c}, & E_c \leq 8 \text{ MeV} \\ p_4 + p_5[1 - e^{-p_6 E_c}] + 0.68, & E_c > 8 \text{ MeV} \end{cases}$$

where  $E_c = E_n + B$  is the excitation energy (in MeV) given by the sum of the incident neutron energy and binding energy (per nucleon), respectively. Since for low excitation energies there are no, or very few, pre-fission neutrons, it is a good approximation to consider  $\nu \approx \nu_F$ , i.e. the average number of prompt neutrons emitted after fission. The set of the parameters used in this work is  $\vec{p} = \{9.18 \cdot$

10<sup>-2</sup>, 1.563, 16.66, 8.04·10<sup>-9</sup>, 2.8, 3.5}. Table A.2 gives the values of the average number of nucleons emitted before and after fission calculated by above equation for  $\nu(E_c, Z_f; \vec{p})$  for 4 actinides at different incident neutron energy. In this section it is also important to mention the quantity  $\nu_p(A)$  that is used to guarantee the complementarity in mass number  $A$  between light- and heavy-fission products, namely

$$A_f = A'_H + A'_L = A_L + \nu_p(A_L) + A_H + \nu_p(A_H) .$$

As described in Ref. [3], the function  $\nu_p$  is the product between the average number of neutrons emitted to form fission products with mass number  $A$  and the fraction of these neutrons that form fission products with  $A$ , respectively, as

$$\nu_p(A) = \nu_t(A, E_c; \nu) R(A) ,$$

where for  $\nu_t$  and  $R(A)$  we used the parameterization given in Ref. [3].

Table A.2. Values of the average number of nucleons emitted before and after fission calculated by the equation for  $\nu(E_c, Z_f; \vec{p})$  for different fissioning nuclei at several neutron incident energies

	0.0253 (eV)	500 (keV)	5 (MeV)	14 (MeV)
<sup>232</sup> Th	2.26	2.32	3.88	4.15
<sup>235</sup> U	2.45	2.51	3.89	4.16
<sup>239</sup> Pu	2.62	2.68	3.89	4.16
<sup>244</sup> Cm	2.77	2.83	3.88	4.15

### A-3. Model for Even-odd Pairing Effects

The following equations describe the parameterization of the function  $F(A)$  describing the even-odd effects in proton and neutron pairing as defined by Wahl [3],

$$F(A; \vec{f}) = \begin{cases} F_Z \cdot F_{A-Z} & Z \text{ even, } A - Z \text{ even} \\ F_Z \cdot F_{A-Z}^{-1} & Z \text{ even, } A - Z \text{ odd} \\ F_Z^{-1} \cdot F_{A-Z} & Z \text{ odd, } A - Z \text{ even} \\ F_Z^{-1} \cdot F_{A-Z}^{-1} & Z \text{ odd, } A - Z \text{ odd,} \end{cases}$$

where the quantities  $F_Z \equiv F_Z(A'; \vec{f})$  and  $F_{A-Z} \equiv F_{A-Z}(A'; \vec{f})$  are expressed by simple functions within the region boundaries  $b$  defined in Sec. A.2 and depending on  $A' = A + \nu_p$ . The parametrization of  $F_Z$  and  $F_{A-Z}$  for excitation energy  $E_c \leq 8$  MeV is given, respectively, by

$$F_Z = \begin{cases} f_{Z140} + f_{\partial F_Z}(b_2 - A') & b_1 \leq A' < b_2 \\ f_{Z140} + f_{\partial F_Z}(A' - b_7) & b_7 < A' \leq b_8 \\ f_5 & b_3 < A' < b_6 \\ f_{Z140} & \text{else} \end{cases}$$

where

$$f_{Z140}(A_f; f_0, f_1, f_2) = \sum_{i=0}^2 f_i (A_f - 236)^i,$$

$$f_{\partial F_Z}(Z_f; f_3, f_4) = f_3 + f_4 (Z_f - 92),$$

and

$$F_{A-Z} = \begin{cases} f_6 + f_7(b_2 - A') & b_1 \leq A' < b_2 \\ f_6 + f_7(A' - b_7) & b_7 < A' \leq b_8 \\ f_8 & b_3 < A' < b_6 \\ f_6 & \text{else} \end{cases}$$

where the vector  $\vec{f} = \{1.207, -0.042, 0.0022, 0.159, -0.028, 1, 1.076, 0.039, 1\}$  contains the values of  $f_0, \dots, f_8$  parameters used to define  $F(A)$ . Table A.3 contains the values of the parameters with related uncertainties for  $^{235}\text{U}$  at thermal neutron incident energy used in the calculations. In this specific case the functions defining parameters such as  $f_{140}$  or  $f_{\partial F_Z}$  are highly simplified since the mass number of the compound nucleus is  $A_f = 236$  and the atomic number  $Z_f = 92$ .

Table A.3. Parameters and related uncertainties defining the functions for  $F_A$  and  $F_{A-Z}$  for  $^{235}\text{U}$  at thermal neutron incident energy

Name	$\bar{f}_r$	$\Delta \bar{f}_r$	Error (%)	Correlation Matrix			
$f_{Z140}$	1.207	$2.414 \cdot 10^{-2}$	2	1.000			
$f_{\partial F_Z}$	0.159	$1.590 \cdot 10^{-3}$	1	0.000	1.000		
$f_6$	1.076	$2.152 \cdot 10^{-2}$	2	0.000	0.000	1.000	
$f_7$	0.039	$3.900 \cdot 10^{-3}$	1	0.000	0.000	0.000	1.000

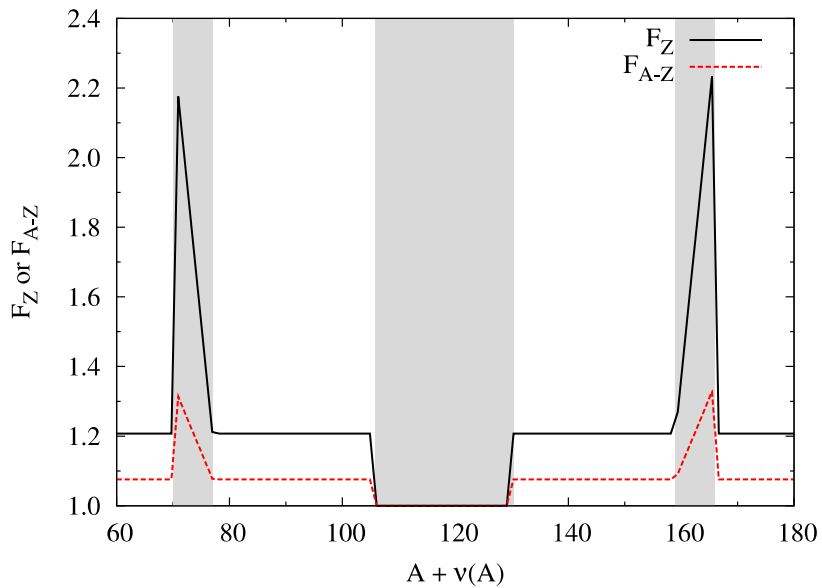


Figure A.1.  $F_Z$  (in solid black) and  $F_{A-Z}$  (in dashed red) functions for  $^{235}\text{U}$  for excitation energy  $E_c \leq 8$  MeV. Highlighted (in gray) are the wing and symmetry boundary regions.

#### A-4. Model for $\sigma_Z$

The following equations define the parameterization of the function  $\sigma_Z \equiv \sigma_Z(A'; \vec{s})$  describing the width of the gaussian charge distribution according to the Wahl's model [3]. For excitation energy  $E_c \leq 8$  MeV, one has

$$\sigma_Z = \begin{cases} s_{Z140} + s_5(A_f - b_2 - 140) & A' < b_1 \\ s_{Z140} + s_{\partial\sigma_Z}(b_2 - A') + s_5(A_f - b_2 - 140) & b_1 \leq A' < b_2 \\ s_{Z140} + s_5(A_f - A' - 140) & b_2 \leq A' < b_3 \\ s_{Z140} + s_5(b_5 - 140) & b_4 \leq A' < b_5 \\ s_{Z140} + s_5(A' - 140) & b_6 \leq A' < b_7 \\ s_{Z140} + s_{\partial\sigma_Z}(A' - b_7) + s_5(b_7 - 140) & b_7 < A' \leq b_8 \\ s_{Z140} + s_5(b_7 - 140) & A' > b_8 \\ s_{Z50} & \text{else} \end{cases}$$

$$s_{Z140}(A_f, E_c; s_0, s_1, s_2) = s_0 + s_1(A_f - 236) + s_2(E_c - 6.551),$$

$$s_{\partial\sigma_Z}(Z_f; s_3, s_4) = s_3 + s_4(Z_f - 92),$$

$$s_{Z50}(Z_f; s_6, s_7) = s_6 + s_7(Z_f - 92).$$

$\vec{s} = \{0.566, 0.0064, 0.0109, -0.045, 0.0094, -0.0038, 0.356, 0.06\}$  is the vector containing the values of the parameters  $s_0, \dots, s_7$ .

Table A.4. Parameters and related uncertainties defining the functions for  $\sigma_Z$  in the case of  $^{235}\text{U}$  at thermal neutron incident energy. The excitation energy used for  $s_{Z140}$  is  $E_c = 7.59$  MeV

Name	$\vec{s}_r$	$\Delta\vec{s}_r$	Error (%)	Correlation Matrix			
$s_{Z140}$	0.5773	$2.886 \cdot 10^{-3}$	0.5	1.000			
$f_{\partial\sigma_Z}$	0.0109	$1.090 \cdot 10^{-4}$	1	0.000	1.000		
$s_5$	-0.0038	$3.800 \cdot 10^{-5}$	1	0.000	0.000	1.000	
$s_{Z50}$	0.3560	$3.560 \cdot 10^{-3}$	1	0.000	0.000	0.000	1.000

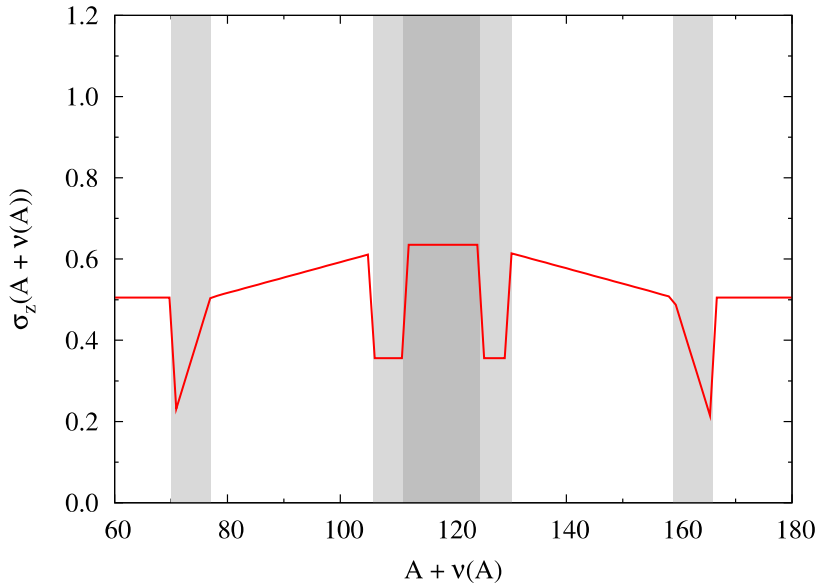


Figure A.2.  $\sigma_Z$  function for  $^{235}\text{U}$  for excitation energy  $E_c \leq 8$  MeV. Highlighted (in gray) are the wing and symmetry boundary regions.

#### A-4. Model for $\Delta Z$

The mean charge of the distribution is corrected by the function  $\Delta Z(A'; \vec{d})$  and its parameterization for excitation energy  $E_c \leq 8$  MeV follows the simple equations.

$$\Delta Z = \begin{cases} -d_{Z140} - d_3(A_f - b_2 - 140) & A' < b_1 \\ -d_{Z140} - d_3(A_f - A' - 140) - d_{\partial\Delta Z}(A' - b_2) & b_1 \leq A' < b_2 \\ -d_{Z140} - d_3(A_f - A' - 140) & b_2 \leq A' < b_3 \\ -d_{Z140} - d_3(A_f - b_3 - 140) - d_5(A' - b_3) & b_3 \leq A' < b_4 \\ \Delta Z(b_4) - (A' - b_4) \frac{\Delta Z(b_5) - \Delta Z(b_4)}{b_4 - b_5} & b_4 < A' < b_5 \\ d_{Z140} + d_3(b_4 - 140) + d_5(b_2 - A') & b_5 \leq A' < b_6 \\ d_{Z140} + d_3(A' - 140) & b_6 \leq A' < b_7 \\ d_{Z140} + d_3(A' - 140) + d_{\partial\Delta Z}(b_7 - A') & b_7 \leq A' \leq b_8 \\ d_{Z140} + s_5(b_7 - 140) & A' > b_8 \end{cases}$$

$$d_{Z140}(A_f; d_0, d_1, d_2) = \sum_{i=0}^2 d_i (A_f - 236)^i,$$

$$d_{\partial\Delta Z}(Z_f; d_4) = d_4 (Z_f - 92).$$

$\vec{d} = \{-0.487, 0.0180, -0.00203, -0.008, -0.0045, 0.191\}$  is the vector containing the values of the parameters  $d_0, \dots, d_6$ . The function  $\Delta Z$  is plotted in Fig. A.6, while Tab. A.5 contains the values of the parameters with related uncertainties for  $^{235}\text{U}$  at thermal neutron incident energy used in the calculations.

Table A.5. Parameters and related uncertainties defining the functions for  $\Delta Z$  in the case of  $^{235}\text{U}$  at thermal neutron incident energy

Name	$\vec{d}_r$	$\Delta\vec{d}_r$	Error (%)	Correlation Matrix	
$d_{Z140}$	-0.487	$1.217 \cdot 10^{-2}$	2.5	1.000	
$d_5$	0.191	$1.910 \cdot 10^{-3}$	1	0.000	1.000

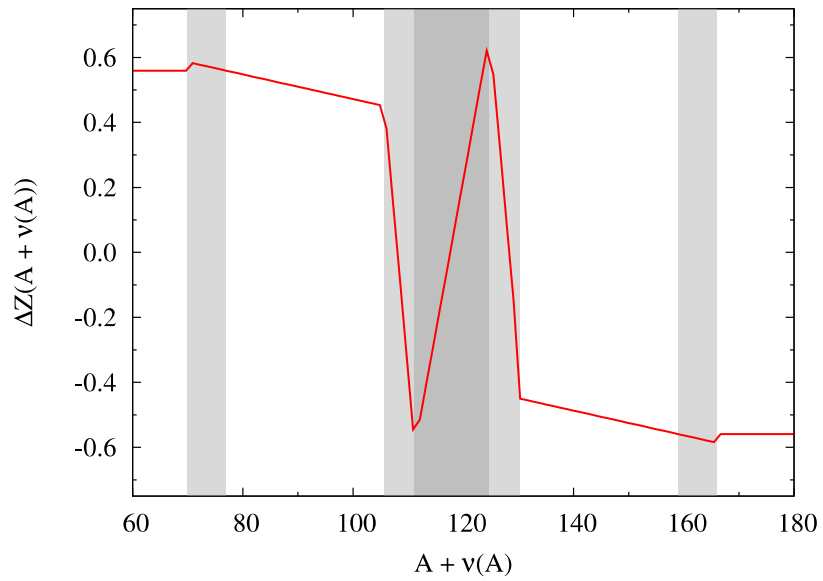


Figure A.3..  $\Delta Z$  function for  $^{235}\text{U}$  for excitation energy  $E_c \leq 8$  MeV. Highlighted (in gray) are the wing and symmetry boundary regions.